Temperature dependence of electrical resistivity in $(Fe_{1-x}Ti_x)_3Al$ alloys

2000 J. Phys.: Condens. Matter 12 9153

(http://iopscience.iop.org/0953-8984/12/43/305)

J. Phys.: Condens. Matter **12** (2000) 9153–9162. Printed in the UK PII: S0953-8984(00)16328-3

Temperature dependence of electrical resistivity in $(Fe_{1-x}Ti_x)_3Al$ alloys

M Kato†, Y Nishino†§, U Mizutani‡, Y Watanabe† and S Asano†

† Department of Materials Science and Engineering, Nagoya Institute of Technology, Showa-ku, Nagoya 466-8555, Japan

‡ Department of Crystalline Materials Science, Nagoya University, Chikusa-ku, Nagoya 464-8603, Japan

Received 14 August 2000

Abstract. We report on the temperature dependence of electrical resistivity in $(Fe_{1-x}Ti_x)_3Al$ alloys with Ti compositions $x = 0$–0.33. Samples in the composition range $0 \leqslant x \leqslant 0.15$ are found to exhibit ferromagnetism with the Curie temperature T_C decreasing from 770 K for $x = 0$ to 145 K for $x = 0.15$. The electrical resistivity below about 400 K for these Ti-poor samples increases rapidly with increasing x, but a negative temperature derivative of resistivity ($d\rho/dT$) dominates above T_C up to 1000 K and above. In contrast, samples in the range $0.20 \leqslant x \leqslant 0.33$ are in a paramagnetic state, at least down to 2 K, and exhibit a rapid decrease in the low-temperature resistivity with increasing Ti composition x. In particular, the Heusler-type Fe_2TiAl ($x = 0.33$) shows a large positive $d\rho/dT$ with the residual resistivity of only about 20 $\mu\Omega$ cm, in sharp contrast to a closely related system Fe_2VAl reminiscent of a semiconductor-like behaviour with the resistivity reaching 3000 $\mu\Omega$ cm at 2 K. This can be explained by the fact that Fe_2TiAl possesses a much higher density of states at the Fermi level than Fe_2VAl, as deduced from the low-temperature specific-heat measurements supplemented by the band calculations in literature. The reason for the possession of a large positive $d\rho/dT$ in Fe_2TiAl is discussed in relation to the Bloch–Grüneisen law.

1. Introduction

The intermetallic compound Fe_3Al is a well ordered ferromagnet with a $D0_3$ crystal structure. We have recently found an anomalous temperature dependence of electrical resistivity in a series of the pseudobinary alloys $(Fe_{1-x}M_x)_3Al$ in which Fe atoms are partly replaced by other 3d transition elements such as M = Ti, V, Cr, and Mn [1, 2]. As reviewed by Nishino [3], these alloys possess general features characterized by (1) a resistance maximum near the Curie point T_C and (2) a negative temperature derivative of resistivity ($d\rho/dT$) at high temperatures above T_C up to 1000 K and above. Such a resistance anomaly tends to appear more strongly with increasing composition x of the substituted element M, in parallel with a sharp reduction in T_C.

The most spectacular feature of the resistance anomaly has been found for $(Fe_{1-x}V_x)_3Al$ [2]. In particular, the Heusler-type Fe_2VAl ($x = 0.33$) is found to be in a marginally magnetic state and to exhibit a semiconductor-like behaviour with the resistivity reaching 3000 $\mu\Omega$ cm at 2 K. This unusual resistivity behaviour is accompanied by the presence of a clear Fermi cutoff in photoemission spectra and an anomalous enhancement in

§ Author to whom any correspondence should be addressed.

0953-8984/00/439153+10$30.00

the electronic specific-heat coefficient at low temperatures. Recent band-structure calculations [4–9] consistently predicted that Fe_2VAl is a nonmagnetic semimetal having a deep pseudogap centred right at the Fermi level E_F. Indeed, nuclear magnetic resonance (NMR) [10, 11] and Hall-effect measurements [12] have confirmed the possession of a very low carrier concentration. Low-temperature specific-heat studies have also demonstrated a substantial decrease in the density of states (DOS) at E_F with the V substitution [13, 14]. More recently, the existence of a pseudogap of 0.1–0.2 eV in width has been experimentally confirmed in Fe_2VAl by optical conductivity measurements [15].

In order to deepen the understanding of the observed unusual transport properties of Fe_2VAl, it is of crucial importance to compare the results with those for systems with the substitution of M other than V. Indeed, electronic band-structure calculations have also been reported for Fe_2TiAl [7, 9]. Botton *et al* [9] noted great similarities in the overall shape of the DOS between Fe_2TiAl and Fe_2VAl, including the possession of a deep pseudogap. However, it must be emphasized here that the Fermi level E_F sits in the middle of the sharp pseudogap in Fe_2VAl whereas E_F substantially shifts from the pseudogap in Fe_2TiAl. As a result, Fe_2TiAl has a very large DOS at E_F, indicating the possession of a metallic band structure, in sharp contrast to a semimetallic nature as in Fe_2VAl. As far as the low Ti composition range ($0 \leqslant x \leqslant 0.15$) is concerned, the electrical resistivity at temperatures below 400 K in $(Fe_{1-x}Ti_x)_3Al$ increases rapidly with increasing x in the same way as that found in $(Fe_{1-x}V_x)_3Al$ [1]. It is, therefore, of great interest to study the resistivity behaviour of Ti-rich samples with $x > 0.15$ including Fe_2TiAl ($x = 0.33$), since the substantial difference in the electronic structure at the Fermi level is most likely reflected in the transport properties. The purpose of the present work is to investigate systematically the temperature dependence of electrical resistivity in $(Fe_{1-x}Ti_x)_3Al$ with $x = 0$–0.33. The low-temperature specific heat was also measured for both Fe_2TiAl and Fe_2VAl to allow a direct comparison of the DOS at the Fermi level between these two Heusler-type compounds. We also discuss why a large positive $d\rho/dT$ dominates in the temperature range roughly below the Debye temperature for Fe_2TiAl on the basis of the Bloch–Grüneisen law.

2. Experiment

2.1. Sample preparation

Ingots of $(Fe_{1-x}Ti_x)_3Al$ alloys with $x = 0$–0.33 were prepared by repeating arc-melting of appropriate amounts of 99.99% pure Fe and Al, and 99.9% pure Ti in an argon gas atmosphere. Since the weight loss after melting was less than 0.3%, the nominal composition was accepted as being accurate. The ingots were homogenized at 1273 K for more than 170 ks in vacuum. Samples were cut from the ingots with a SiC blade saw to the size of $1 \times 1 \times 15$ mm^3 for resistivity measurements, and $7 \times 7 \times 15$ mm^3 for specific heat measurements. Each sample was sealed in an evacuated quartz capsule and was annealed at 1273 K for 3.6 ks and then at 673 K for 14.4 ks followed by furnace cooling. This sample preparation is the same as employed previously for $(Fe_{1-x}V_x)_3Al$ [2, 12, 14]. Further, as will be discussed later, some of Ti-rich samples with $x \geqslant 0.20$ were quenched into water after annealing at 1073 K for 18 ks.

2.2. Measurements

X-ray diffraction spectra were taken with Cu Kα radiation on powdered samples prepared as above. The electrical resistivity was measured by a standard d.c. four-terminal method with a current of 100 mA over the temperature range from 4.2 to 1373 K: the measurements at high

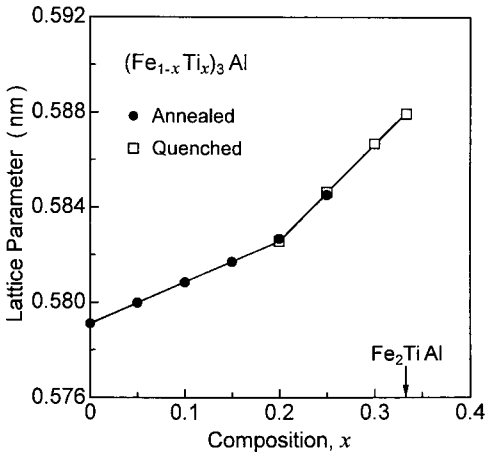

Figure 1. Lattice parameter as a function of Ti composition x in $(Fe_{1-x}Ti_x)_3Al$. The solid circles and open squares represent the data on annealed and quenched samples, respectively.

temperatures were carried out in a vacuum of 4×10^{-4} Pa with a rising rate of 0.05 K s^{-1}. The specific heat was measured by using the d.c. adiabatic method from 1.5 to 25 K. The Curie temperature was determined from thermomagnetic measurements using a superconducting quantum interference device (SQUID) magnetometer and also by means of differential thermal analysis.

3. Results

3.1. X-ray diffraction analysis

The x-ray diffraction measurements could identify annealed samples of $(Fe_{1-x}Ti_x)_3Al$ to be in a single-phase $D0_3$ structure in the composition range $0 \leqslant x \leqslant 0.25$. However, a small amount of an additional phase, probably the Laves phase (Fe_2Ti), was detected for $x \geqslant 0.30$. The volume fraction of the Laves phase was estimated by comparing the peak intensities of x-ray diffraction and was found to be approximately 0.2 and 3.0 vol% for $x = 0.30$ and 0.33, respectively. On the other hand, the $D0_3$ single phase was maintained up to $x = 0.30$ for quenched samples, while the amount of the Laves phase was reduced to only 1.1 vol.% for $x = 0.33$ (Fe_2TiAl).

The lattice parameter of the $D0_3$ phase is plotted in figure 1 as a function of the Ti composition x in $(Fe_{1-x}Ti_x)_3Al$. The lattice parameters of annealed samples shown by solid circles almost coincide with those of quenched samples ($x = 0.20$ and 0.25) shown by open squares. The lattice parameter increases with increasing x, but the lattice dilatation is much smaller than that estimated from the Fe–Ti primary (bcc) solid solution [16]. This suggests that the substitution of Ti substantially contracts the lattice spacing as a result of the distinctive stabilization of the $D0_3$ phase. The lattice parameter of the quenched Fe_2TiAl sample is equal to 0.588 nm, being in good agreement with the earlier report [17], in which the formation of Fe_2TiAl with the Heusler-type ($L2_1$) structure has been confirmed by neutron diffraction. We believe that the transport properties of the quenched Fe_2TiAl sample would be practically unaffected by the presence of a very small amount of the unavoidable Laves phase.

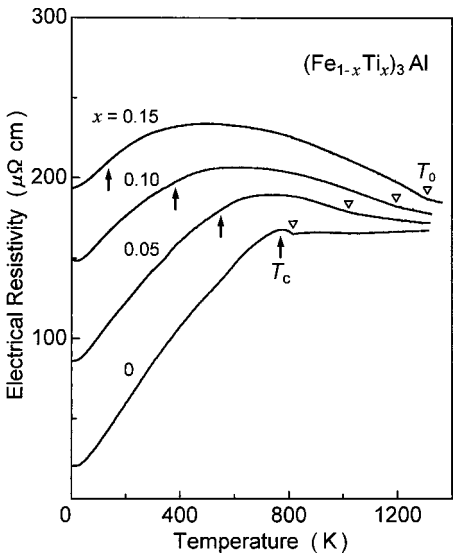

Figure 2. Temperature dependence of electrical resistivity in $(Fe_{1-x}Ti_x)_3Al$ for low Ti compositions $x = 0$–0.15. The arrows denoted by T_C indicate the Curie temperatures. The open triangles denoted by T_0 indicate the $D0_3$–B2 transformation temperatures.

3.2. Electrical resistivity

Figure 2 shows the temperature dependence of the electrical resistivity in $(Fe_{1-x}Ti_x)_3Al$ for low Ti compositions $x = 0$–0.15. These curves were obtained on both heating and cooling runs, which almost coincided with each other. The arrow denoted by T_C indicates the Curie temperature. The value of T_C for $x = 0.15$ was determined by the thermomagnetic measurements in magnetic fields up to 5 T, using a modified Arrott plot method, and was found to be 145 K. We see from figure 2 that, upon substitution of Ti for Fe, the electrical resistivity in the low temperature range increases rapidly but tends to saturate and forms a maximum at temperatures above T_C with the subsequent decrease with further increase in temperature. In parallel with a sharp decrease in T_C, the resistance maximum is shifted to a lower temperature. A similar resistance maximum has also been reported to occur in engineered alloys of Fe_3Al containing Ti and Mo [18]. The magnitude of the observed negative $d\rho/dT$ at higher temperatures increases as the Ti composition x increases, which is consistent with our earlier report [1]. The negative $d\rho/dT$ has also been observed for Fe_3Ga- [19] and Fe_3Si-based alloys [20] with the substitution of Ti for Fe. Also noted in figure 2 is that the resistivity curves show an inflection at temperatures above 800 K, as indicated by open triangles denoted by T_0. This inflection is known to be caused by the $D0_3$–B2 phase transformation and, hence, the transformation temperature can be precisely determined from it. The transformation temperature increases remarkably with increasing Ti composition at the rate of 50–55 K/at. %Ti, as already reported in previous investigations [1, 21–25].

Figure 3 shows the temperature dependence of the electrical resistivity in $(Fe_{1-x}Ti_x)_3Al$ for high Ti compositions $x = 0.15$–0.33: the curve for $x = 0.15$ is the same as that shown in figure 2. Note here that the Arrott plots for $x \geqslant 0.20$ did not show any evidence of a ferromagnetic transition, although the magnetizations measured under a magnetic field of 1.0 T were still enhanced at low temperatures at least down to 2 K. We believe, therefore, that

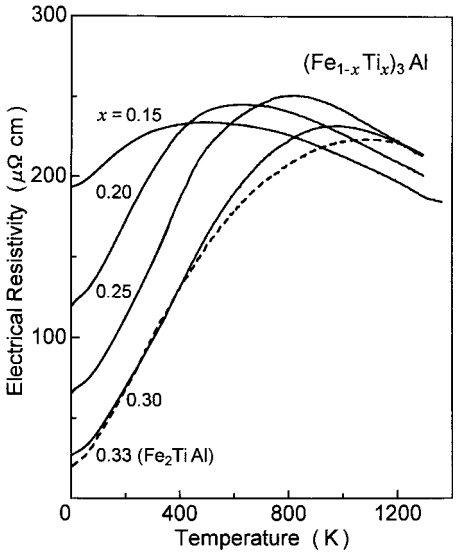

Figure 3. Temperature dependence of electrical resistivity in $(Fe_{1-x}Ti_x)_3Al$ for high Ti compositions $x = 0.15$–0.33. The resistivity curve for the quenched Fe_2TiAl sample ($x = 0.33$) is shown by the dashed line.

Ti-rich alloys with $x \geqslant 0.20$ are in a paramagnetic state over the whole temperature range examined. The resistivity curves were measured on annealed samples for $0.15 \leqslant x \leqslant 0.25$ and on quenched samples for $x = 0.30$ and 0.33. It may be worthwhile mentioning that resistivity curves for quenched samples with $x = 0.20$ and 0.25 were similar to those shown in figure 3 but their residual resistivities were always slightly higher than those in annealed ones owing to the existence of vacancies introduced by quenching. In striking contrast to the results in figure 2, the electrical resistivity decreases significantly at low temperatures as the Ti composition x exceeds 0.15, resulting in widening of the temperature range having a positive $d\rho/dT$. The resistivity curves of Ti-rich samples again clearly tend to saturate at higher temperatures and form a broad maximum for all samples studied. In particular, the Heusler-type Fe_2TiAl shows the smallest residual resistivity of only about 20 $\mu\Omega$ cm, but a large positive $d\rho/dT$ is responsible for an increase in resistivity up to above 200 $\mu\Omega$ cm in the temperature range above about 800 K.

3.3. Specific heat

We measured the low-temperature specific heat of Fe_2TiAl and Fe_2VAl in order to compare their DOSs at the Fermi level. In figure 4, the specific heat C is shown in the ordinary form of C/T against T^2. Note here that the present value of C is defined in units of per mole atom and should be multiplied by a factor of four when expressed in units of 'chemical formula' moles. It is seen that the specific heat of Fe_2TiAl is definitely higher than that of Fe_2VAl over the whole temperature range studied. Remarkably, C/T for Fe_2TiAl, as well as for Fe_2VAl, is found to be enhanced significantly with decreasing temperature below 10 K. We believe that the observed upturn in C/T at low temperatures is due to strong spin fluctuations associated with nonstoichiometry or with antisite defects, as suggested by Singh and Mazin [5]. The low-temperature upturn for Fe_2VAl has also been discussed in term of a Schottky anomaly arising from magnetic clusters [13].

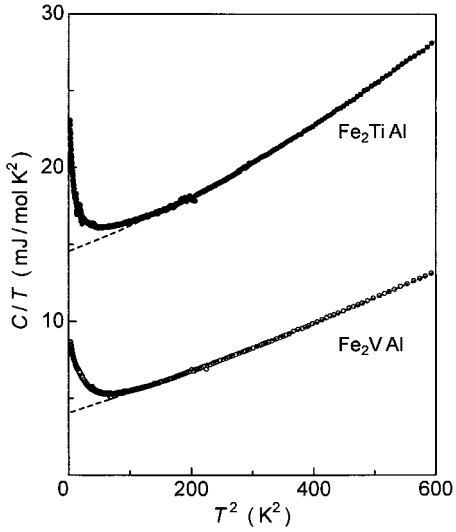

Figure 4. Specific heat over temperature, C/T, versus T^2 measured for Fe_2TiAl (dots) and Fe_2VAl (circles). The dashed curves represent a least squares fitting to equation (1).

Although the electronic specific-heat coefficient is strongly temperature dependent at low temperatures, C/T increases almost linearly with T^2 in the temperature range above 10 K, as is clearly seen in figure 4. The specific heat at higher temperatures is believed to be composed of a combination of electronic and lattice contributions. We fit the data in the range 10 and 25 K to the ordinary equation

$$C = \gamma T + \alpha T^3 + \delta T^5 \tag{1}$$

where the first term represents the electronic specific heat and the remaining two the lattice contributions [26]. The electronic specific-heat coefficient γ was determined by a least squares fitting, as shown by the dotted curves in figure 4: $\gamma = 12.7$ mJ mol^{-1} K^{-2} for Fe_2TiAl and $\gamma = 3.9$ mJ mol^{-1} K^{-2} for Fe_2VAl. The measured value of γ for Fe_2VAl is very close to that deduced from the electronic specific-heat data at 6 K [14], but is still larger than that reported by Lue *et al* [13]. Note that the electronic specific-heat coefficient deduced from the band calculations for Fe_2VAl is only 0.2 mJ mol^{-1} K^{-2} [4] and is much smaller than the experimental value because of the mass enhancement effect discussed previously [2, 14]. Similarly we found that the measured value of γ for Fe_2TiAl is larger by a factor of three or four than the calculated one [7, 9]. Apart from this discrepancy, we could confirm experimentally from the specific heat measurements that the DOS at the Fermi level, $N(E_F)$, of Fe_2TiAl is about three times as high as that of Fe_2VAl as a result of the shift of the Fermi level off from the centre of the pseudogap.

The least squares fitting also determines the lattice specific-heat coefficient, α, which can be related to the Debye temperature θ_D as follows:

$$\theta_D = (12\pi^4 R/5\alpha)^{1/3} \tag{2}$$

where R is the gas constant. We obtained $\theta_D = 425$ K for Fe_2TiAl and $\theta_D = 510$ K for Fe_2VAl. The value of θ_D for Fe_2VAl agrees well with that extrapolated from those for $(Fe_{1-x}V_x)_3Al$ in our previous study [14]. Both the θ_D values for Fe_2TiAl and Fe_2VAl are higher than that for Fe_3Al, i.e. $\theta_D = 377$ K [14], suggesting a substantial enhancement of the atomic bonding in the Heusler structure.

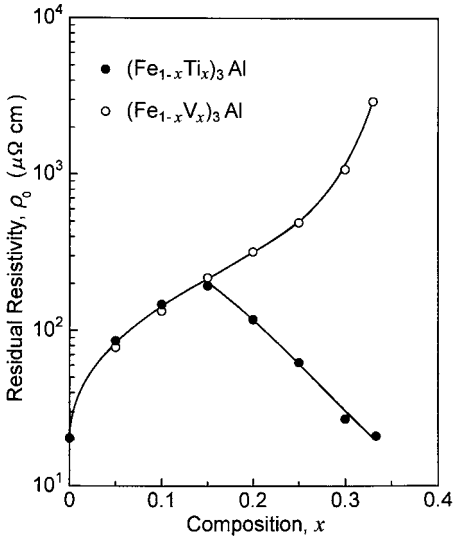

Figure 5. Residual resistivity ρ_0 as a function of Ti and V compositions x in $(Fe_{1-x}Ti_x)_3Al$ (solid circles) and $(Fe_{1-x}V_x)_3Al$ (open circles), respectively.

4. Discussion

4.1. Saturation effect in the temperature dependence of resistivity

We discuss first why the resistivity tends to saturate and a negative $d\rho/dT$ occurs at high temperatures. Indeed, this is a quite universal feature observed for many crystalline and amorphous alloys and intermetallic compounds, and a positive $d\rho/dT$ switches to a negative one when the resistivity exceeds about 200 $\mu\Omega$ cm. This phenomenon is often referred to as Mooij's criterion [27]. As has been discussed by Mizutani [28], an increase in resistivity with increasing temperature is brought about by the reduction in the electron mean free path and the Boltzmann transport mechanism fails when its value becomes comparable to the interatomic distance. This condition is generally fulfilled when the resistivity reaches about 150–200 $\mu\Omega$ cm. As will be discussed further in section 4.3, we believe that the mechanism for the appearance of a positive $d\rho/dT$ at temperatures, say, below the Debye temperature is caused by a decreasing mean free path due to increasing electron–phonon interaction with increasing temperature. This means that the saturation effect observed in the present alloys can be taken as the termination of the mean free path effect. The saturation effect does not necessarily mean the occurrence of a negative $d\rho/dT$ at the highest temperature range where the measuring temperature far exceeds the Debye temperature. Here the elastic scattering of electrons with ions is expected to dominate in the same way as in liquid metals, where the occurrence of a negative $d\rho/dT$ is often discussed in relation to the Ziman theory [29]. Of course, we cannot directly apply the Ziman theory to a crystal metal as in the present case. Further discussion on the occurrence of a negative $d\rho/dT$ in a crystal at very high temperatures like 1200 K is still premature at this stage.

4.2. Composition dependence of residual resistivity

The residual resistivity ρ_0 is shown in figure 5 as a function of the Ti composition x in $(Fe_{1-x}Ti_x)_3Al$: the logarithm of resistivity is plotted on the ordinate. Also shown in this

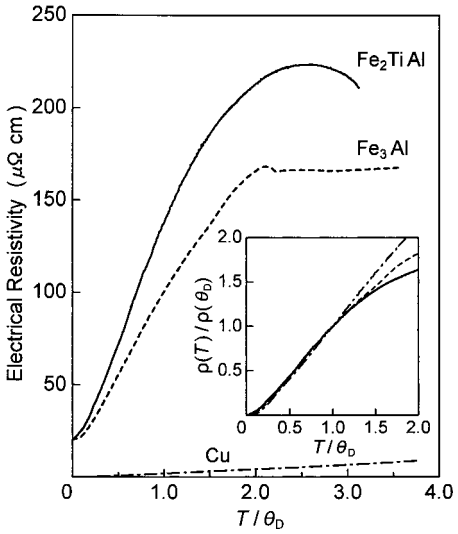

Figure 6. Electrical resistivity as a function of the temperature which is normalized by the respective Debye temperatures, T/θ_D, for Fe_2TiAl (solid curve), Fe_3Al (dashed curve) and pure Cu (dash–dotted curve). The inset shows the relation between $\rho(T)/\rho(\theta_D)$ and T/θ_D for the three systems: $\rho(T)$ represents the temperature-dependent electron–phonon contribution. The Debye temperatures for Fe_2TiAl, Fe_3Al and pure Cu are chosen to be 425, 377 and 342 K, respectively.

figure are the ρ_0 values for $(Fe_{1-x}V_x)_3Al$ taken from our data reported earlier [12, 14]. In the composition range $0 \leqslant x \leqslant 0.15$, the residual resistivity increases with increasing x in the same manner as that for the V substitution. However, the ρ_0 value turns out to decrease sharply for $x > 0.15$ and is reduced to only 20 $\mu\Omega$ cm at $x = 0.33$ (Fe_2TiAl). In contrast, the residual resistivity in $(Fe_{1-x}V_x)_3Al$ increases continuously with increasing x and reaches about 3000 $\mu\Omega$ cm at $x = 0.33$ (Fe_2VAl). We can attribute the observed large difference in the resistivity behaviour between Fe_2TiAl and Fe_2VAl to the difference in the DOS at the Fermi level, as discussed in section 3.3.

It should be remarked in figure 5 that the x-dependence of the residual resistivity in $(Fe_{1-x}Ti_x)_3Al$ exhibits a maximum at $x = 0.15$. As discussed by Weinert and Watson [7], the presence of a hybridization pseudogap may be regarded as a common feature in transition-metal aluminides including both Fe_2VAl and Fe_2TiAl. They suggested that the Fermi level falls in the pseudogap when there are five 3d electrons per transition-metal atom, i.e. 15 3d electrons in the three transition-metal spheres for the present Heusler-type compounds. In fact, since the total number of 3d electrons is equal to 15 for Fe_2VAl, the Fermi level falls right at the centre of the pseudogap. However, the total number of 3d electrons is equal to 14 for Fe_2TiAl. Hence, the Fermi level is shifted off from the centre of the pseudogap and, according to the band calculations [7, 9], it is located at an energy approximately 0.5 eV below the pseudogap. A simple manipulation yields a total of exactly 15 3d electrons per chemical formula unit when $x = 0.25$. This would roughly explain why the residual resistivity exhibits a maximum at an intermediate Ti composition. Finally, it is noted that a similar Ti composition dependence of the residual resistivity has been observed in $(Fe_{1-x}Ti_x)_3Ga$ [19].

4.3. Temperature dependence of resistivity in Fe_2TiAl

As emphasized earlier, we have observed a large positive $d\rho/dT$ at temperatures below approximately the Debye temperature in the present $(Fe_{1-x}Ti_x)_3Al$ alloys. The electrical

resistivity data for the three representative systems Fe_2TiAl, Fe_3Al and pure Cu are plotted in figure 6 as a function of the temperature, which is normalized with respect to the respective Debye temperatures, T/θ_D. It is seen that the value of $d\rho/dT$ for Fe_2TiAl and Fe_3Al is much larger than that of Cu, which is shown by the dash–dotted curve. Moreover, the saturation effect can be clearly observed for both Fe_3Al and Fe_2TiAl, the origin of which has been discussed in section 4.1. First, the temperature-independent impurity scattering contribution is subtracted from the measured total resistivity. The resulting $\rho(T)$ data represent the temperature-dependent electron–phonon contribution and may be well analysed by using the well known Bloch–Grüneisen law [29]. The inset to figure 6 shows the relation between $\rho(T)/\rho(\theta_D)$ and T/θ_D. Surprisingly, all the curves coincide quite well in the temperature range $T \leqslant \theta_D$, whereas the data in the range $T > \theta_D$ for Fe_2TiAl and Fe_3Al show strong downward deviation from a linear dependence observed for Cu due to the saturation effect discussed above. The inset to figure 6 implies that the electron–phonon contribution to the resistivity in the range $T \leqslant \theta_D$ is essentially the same irrespective of the alloy systems. It is also interesting to note that the Bloch–Grüneisen law holds equally well for both ferromagnetic Fe_3Al and paramagnetic Fe_2TiAl, suggesting the electron–magnon interaction to be of minor importance.

We are now ready to consider why a large positive $d\rho/dT$ occurs for Fe_2TiAl and Fe_3Al, as is seen in figure 6. As is clear from the argument above, we can equally address the question to why $\rho(\theta_D)$ for Fe_2TiAl is much larger than that for Cu. In general, the electrical resistivity of an isotropic metallic system can be expressed as follows:

$$\frac{1}{\rho} = \frac{e^2}{3}\Lambda_F v_F N(E_F) \tag{3}$$

where Λ_F is the mean free path and v_F is the Fermi velocity. Here the product of $v_F N(E_F)$ is purely electronic in origin and has very little to do with the temperature dependence of resistivity, which, instead, obviously arises from that of the mean free path. As discussed above in relation to the inset to figure 6, $d\Lambda_F^{-1}/dT$ is essentially the same among the three systems shown there. According to equation (3), we see that the magnitude of $d\rho/dT$ is biased by the magnitude of the coefficient $v_F N(E_F)$. A free-electron-like large value of v_F for Cu is definitely responsible for the possession of a low $d\rho/dT$ as shown in figure 6. In contrast, the value of v_F must be small enough to enhance $d\rho/dT$ for Fe_2TiAl and Fe_3Al because of the location of the Fermi level in the 3d-transition-metal band. The averaged Fermi velocity may be evaluated by taking the derivative of the energy dispersion curve with respect to the wavevector in different directions at the Fermi energy and averaging them over the Fermi surface. Such band calculations are now in progress in order to calculate the product of $v_F N(E_F)$ in the Heusler-type Fe_2TiAl compound.

5. Conclusions

The temperature dependence of electrical resistivity has been investigated for $(Fe_{1-x}Ti_x)_3Al$ alloys with Ti compositions $x = 0$–0.33. In the low Ti composition range ($0 \leqslant x \leqslant 0.15$), the electrical resistivity increases rapidly at low temperatures with increasing x, showing a resistance maximum at temperatures above T_C. In contrast, samples with Ti compositions $x = 0.20$–0.33 are in a paramagnetic state and exhibit a rapid decrease in the low-temperature resistivity with increasing x. In particular, the Heusler-type Fe_2TiAl shows the smallest residual resistivity of only about 20 $\mu\Omega$ cm, but a large positive $d\rho/dT$ is responsible for an increase in resistivity above 200 $\mu\Omega$ cm at high temperatures, where the resistivity saturates and a negative $d\rho/dT$ occurs in accord with the Mooij criterion. By analysing the $\rho(T)$ data on the

basis of the Bloch–Grüneisen law, we could point out that the Fermi velocity must be small enough to cause a large positive $d\rho/dT$ for Fe_2TiAl.

The resistivity behaviour of Fe_2TiAl mentioned above is in sharp contrast to a closely related system Fe_2VAl, which shows a semiconductor-like behaviour with a resistivity reaching 3000 $\mu\Omega$ cm at 2 K. The observed large difference in the resistivity behaviour can be attributed to the fact that Fe_2TiAl possesses a much higher DOS at the Fermi level than Fe_2VAl, as confirmed by the low-temperature specific-heat measurements. Thus, the present results strengthen our previous conclusion that unique transport properties observed for Fe_2VAl originate from the possession of low carrier concentrations as a result of the location of the Fermi level at the centre of the deep pseudogap in the presence of spin fluctuation effects.

Acknowledgments

The authors are grateful to Dr T Biwa and Dr T Takeuchi for their assistance and discussion throughout this work. Thanks are also due to the Research Centre for Molecular Materials, Institute for Molecular Science, for assistance in obtaining the magnetization data.

References

[1] Nishino Y, Kumada C and Asano S 1997 *Scr. Mater.* **36** 461
[2] Nishino Y, Kato M, Asano S, Soda K, Hayasaki M and Mizutani U 1997 *Phys. Rev. Lett.* **79** 1909
[3] Nishino Y 1998 *Mater. Sci. Eng.* A **258** 50
[4] Guo G Y, Botton G A and Nishino Y 1998 *J. Phys.: Condens. Matter* **10** L119
[5] Singh D J and Mazin I I 1998 *Phys. Rev.* B **57** 14 352
[6] Weht R and Pickett W E 1998 *Phys. Rev.* B **58** 6855
[7] Weinert M and Watson R E 1998 *Phys. Rev.* B **58** 9732
[8] Bansil A, Kaprzyk S, Mijnarends P E and Tobola J 1999 *Phys. Rev.* B **60** 13 396
[9] Botton G A, Nishino Y and Humphreys C J 2000 *Intermetallics* at press
[10] Lue C S and Ross J H Jr 1998 *Phys. Rev.* B **58** 9763
[11] Lue C S and Ross J H Jr 2000 *Phys. Rev.* B **61** 9863
[12] Kato M, Nishino Y, Asano S and Ohara S 1998 *J. Japan. Inst. Met.* **62** 669
[13] Lue C S, Ross J H Jr, Chang C F and Yang H D 1999 *Phys. Rev.* B **60** R13 941
[14] Kato M, Nishino Y, Mizutani U and Asano S 2000 *J. Phys.: Condens. Matter* **12** 1769
[15] Okamura H *et al* 2000 *Phys. Rev. Lett.* **84** 3674
[16] Pearson W B 1958 *A Handbook of Lattice Spacings and Structures of Metals and Alloys* (London: Pergamon)
[17] Okpalugo D E, Booth J G and Faunce C A 1985 *J. Phys. F: Met. Phys.* **15** 681
[18] Hyde T A, Sellers C H, Wright J K and Wright R N 1994 *Scr. Metall. Mater.* **30** 113
[19] Kawamiya N, Nishino Y, Matsuo M and Asano S 1991 *Phys. Rev.* B **44** 12 406
[20] Nishino Y, Inoue S, Asano S and Kawamiya N 1993 *Phys. Rev.* B **48** 13 607
[21] Mendiratta M G, Ehlers S K and Lipsitt H A 1987 *Metall. Trans.* A **18** 509
[22] Fortnum R T and Mikkola D E 1987 *Mater. Sci. Eng.* **91** 223
[23] Sellers C H, Hyde T A, O'Brien T K and Wright R N 1994 *J. Phys. Chem. Solids* **55** 505
[24] Anthony L and Fultz B 1995 *Acta Metall. Mater.* **43** 3885
[25] Ohnuma I, Schön C G, Kainuma R, Inden G and Ishida K 1998 *Acta Mater.* **46** 2083
[26] Cezairliyan A 1988 *Specific Heat of Solids* (New York: Hemisphere)
[27] Mooij J H 1973 *Phys. Status Solidi* a **17** 521
[28] Mizutani U 1991 *Phys. Status Solidi* b **176** 9
[29] Ziman J M 1960 *Electrons and Phonons* (London: Oxford University Press)